Pulsed EPR Studies of Doublet Signal and Singlet-like Signal in Oriented Ca^{2+}-Depleted PS II Membranes: Location of the Doublet Signal Center in PS II†

Hiroyuki Mino,*,‡ Asako Kawamori,§ and Taka-aki Ono‡

Laboratory for Photo-Biology, RIKEN Photodynamics Research Center, The Institute of Physical and Chemical Research, 519-1399 Aoba, Aramaki, Aoba, Sendai 980-0845, Japan, and Faculty of Science, Kwansei Gakuin University, 1-1-155 Uegahara, Nishinomiya 662-8501, Japan

Received December 23, 1999; Revised Manuscript Received June 29, 2000

ABSTRACT: Doublet signal and singlet-like signal induced in Ca^{2+}-depleted PS II were investigated by pulsed EPR in one-dimensionally oriented photosystem (PS) II membranes. The doublet signal showed marked angular dependent change in its spectrum in term of the applied magnetic field, indicating that the magnetic dipole−dipole interaction is mainly responsible for the doublet signal. The singlet-like signal also showed angular dependence, which was less pronounced than that of the doublet signal. The parameters of dipole and exchange interactions used to simulate the doublet signal indicate that the signal arises from a magnetically coupled organic radical pair. Angular dependence of the doublet signal indicates that the radius vector of the radical pair (***r***) and the normal of the thylakoid membrane is at an angle of 65°. Pulsed ELDOR studies in the oriented membranes indicate that the vector (***R***) connecting the doublet-signal center with the $Y_D^{\bullet}$ radical and the plane of the thylakoid membrane are at an angle of 8°. Furthermore, the angle between the projections of the ***R*** and ***r*** vectors on the plane of the thylakoid membrane was determined to be 64°. The location of the doublet-signal species in PS II is discussed.

Photosynthetic oxygen evolution is carried out by an oxygen-evolving complex (OEC)[1] containing a tetra-nuclear Mn-cluster located at the lumenal side of PS II protein complexes. Oxidized equivalents generated in the PS II reaction center by the successive absorption of four photons are accumulated on the Mn-cluster and are used for water oxidation. Kinetical analyses have revealed that a molecular oxygen is produced by a series of reactions with five distinct intermediate states labeled S_i ($i = 0-4$), in which S_1 is thermally stable in the dark. By absorbing each photon, the S_1 state advances stepwise to reach the S_4 state that is the highest oxidation state, which decays spontaneously to the S_0 state with the concurrent release of a molecular oxygen (reviewed in refs *1*−*4*). The S-state transitions are accompanied by periodic changes in the oxidation state of the Mn-cluster (*5*, *6*), although the valences of manganese ions in the respective S-states still remain a matter of debate.

Calcium is an indispensable metal cofactor for the normal function of OEC. An X-ray absorption study has demonstrated the presence of Ca^{2+} in close vicinity to the Mn-cluster (*7*). It has been proposed that Ca^{2+} is associated with the Mn-cluster presumably through a carboxylate bridge (*8*) and that Ca^{2+} depletion directly affects the electronic structure of the Mn-cluster (*9*). Oxygen evolution is inhibited by selective depletion of Ca^{2+} and is restored by reconstitution of Ca^{2+}. The formation of the S_2 state in Ca^{2+}-depleted PS II has been depicted by the generation of a multiline EPR signal, the spectral features of which depend on the procedures conducted for Ca^{2+}-depletion (*10*−*13*). Upon illuminating the Ca^{2+}-depleted PS II in the S_2 state, another EPR signal with a splitting line width of 160 G is generated around $g = 2$ by CW EPR (*14*). This split signal has been called "S_3'-state signal", but it may not directly associate to the normal S_3 state that shows a completely different EPR signal (*15*). The S_3'-state signal arises from an unknown auxiliary redox reaction in PS II due to an interruption in the normal oxidation process beyond the S_2 state in the absence of Ca^{2+}. A similar $g = 2.0$ split signal has been induced by illuminating acetate-treated PS II membranes (*16*).

The $g = 2.0$ split signal has been thought to arise from an organic radical with $S = {}^1/_2$ interacting with the S_2-state Mn-cluster, where an oxidized histidine (*17*, *18*) or Y_Z tyrosine (*16*) is attributed to the putative radical. Involvement of the $Y_Z^{\bullet}$ radical in the split signal has been supported by pulsed ENDOR and ESEEM studies (*19*−*21*). The signal has been interpreted to be the interaction between the $Y_Z^{\bullet}$ radical and the oxidized Mn-cluster with $S = 1$ (*19*). This interpretation is based on simulation of the ESE-field swept spectrum in Ca^{2+}-depleted PS II, with an interdistance of 4.5 Å between both species (*19*). An alternative interpretation is that the signal accounts for the interaction between the $Y_Z^{\bullet}$ radical and the S_2-state Mn-cluster with $\boldsymbol{S} = {}^1/_2$. This is based on

† This research was supported by grants for Frontier Research System at RIKEN given by the STA of Japan, and by Grant-in-Aid for Encouragement of Young Scientist (no. 11780433) from the MESSC of Japan. A.K. received financial support from the Hyogo Science and Technical Association Foundation.

* To whom correspondence should be addressed. Fax:+81-22-228-2045. E-mail: mino@postman.riken.go.jp.

‡ RIKEN Photodynamics Research Center.

§ Kwansei Gakuin University.

[1] Abbreviations: Mes, 2-morpholinoethanesulfonic acid; Mops, 4-morpholinopropanesulfonic acid; DCMU, 3-(3,4-dichlorophenyl)-1,1-dimethylurea; ENDOR, electron nuclear double resonance; ESEEM, electron spin−echo envelope modulation; ESE, electron spin−echo; ELDOR, electron electron double resonance; OEC, oxygen-evolving complex; CW, continuous-wave.

10.1021/bi9929406 CCC: $19.00
Published on Web 08/12/2000

simulation of the ESE field-swept spectrum in acetate-treated PS II, where the distance between the two species was assumed to be 3.5 Å (*21*). The involvement of the Mn-cluster in the split signal has been supported by results of high-frequency pulsed ENDOR study that shows the presence of manganese ion signal in the split signal in acetate-treated PS II, where the distance between the Y_Z tyrosine and Mn-cluster was estimated to be between 8.6 and 11.5 Å (*22*). The suggestion that the Y_Z tyrosine is present in close proximity to the Mn-cluster seems to be compatible with a proton abstraction model for water oxidation (*23*).

In these studies, the split signal has been analyzed by assuming that the signal arises from a single magnetic species. However, it has been revealed that the split signal consists of two different signals that overlap at the $g = 2$ region: a symmetric doublet signal and a singlet-like signal. The former signal has a splitting of approximately 150 G at $g = 2$ and is induced by illuminating the Ca^{2+}-depleted PS II in the S_2 state for a short period at 273 K, while the latter signal is induced by a longer illumination period (*19*, *24*). Distinctly, the presence of DCMU did not inhibit the formation of the doublet signal but inhibited that of the singlet-like signal, indicating that the latter signal requires at least two turnovers of PS II beyond the S_2 state. The doublet signal has been simulated by assuming $D_0 = 130$ G and $J = (-)40$ G, which are consistent with its characteristic spectral features that are typical of the interaction between paired organic radicals (*24*). However, the origin of the singlet-like signal remains equivocal. Pulsed ENDOR-induced EPR study indicates that the $Y_Z^{\bullet}$ radical is associated with the doublet signal, but not with the singlet-like signal (*24*).

In the present study, we measured the magnetic anisotropy of the doublet and singlet-like signals in partially oriented PS II membranes. The doublet signal showed marked orientation dependence, indicating that a dipole−dipole interaction between two organic radicals mainly attributed to the signal in consistent with the assumed magnetic parameters for the simulation of the doublet signal (*24*). The ELDOR results provide information on the relative orientation of the putative radical pair and the $Y_D^{\bullet}$ radical with respect to the thylakoid membrane. On the basis of the present and previously reported results, the location of the putative radicals for the doublet signal in PS II is evaluated.

MATERIALS AND METHODS.

Sample Preparations. Oxygen-evolving PS II membranes were prepared from spinach as described in a previous study (*25*) with subsequent modifications (*26*). The membranes were washed twice with a solution containing 400 mM sucrose, 20 mM NaCl, and 0.1 mM Mes/NaOH (pH 6.5) and resuspended in the same buffer solution. For Ca^{2+} depletion, the membranes were suspended in a medium containing 400 mM sucrose, 20 mM NaCl, and 10 mM citric acid/NaOH (pH 3.0) at 0 °C for 5 min, and then, 10% vol of a solution containing 400 mM sucrose, 20 mM NaCl, and 500 mM Mops/NaOH (pH 7.5) was added to adjust the final pH to approximately 6.5 as described in ref *27*. The treated membranes were washed and resuspended in a final buffer solution containing 400 mM sucrose, 20 mM NaCl, and 20 mM Mes/NaOH (pH 6.5). All procedures were carried out in the dark or under a dim green light to maintain the OEC in the S_1 state unless otherwise stated. Ca^{2+}-depleted PS II membranes were collected by centrifugation at 35000*g* for 20 min and were suspended in a buffer solution containing 400 mM sucrose, 20 mM NaCl, 0.5 mM EDTA, and 20 mM Mes/NaOH (pH 6.5). The membrane suspensions were partially dried on pieces of Mylar sheet for 12 h at 4 °C under a wet N_2 stream (*28*). Six to eight pieces of Mylar sheets coated with oriented PS II membranes, were put into an EPR tube. The EPR tubes were purged with Ar gas, sealed, and then stored in liquid N_2 until use.

Pulsed EPR Measurements. Electron spin−echo experiments were performed using a Bruker ESP-380 pulsed EPR spectrometer equipped with a cylindrical dielectric cavity (ER4117DHQ-H, Bruker) and a gas flow-temperature control system (CF935, Oxford Instruments). Microwave (m.w.) pulses of 16 and 24 ns duration for $\pi/2$ and π pulses were used for a 2-pulse (primary) ESE sequence. ESE field-swept spectra were measured using the 2-pulse sequence with a time interval of 200 ns between the m.w. pulses. For ESE ELDOR measurements, a 2 + 1 pulse sequence was used, where m.w. pulses of 16, 24, and 24 ns duration were provided for the spin rotation angles of $\pi/2$, π, and π, respectively. A microwave synthesizer (HP83751A, Hewlett-Packard) was used as a second m.w. source. The output of the synthesizer was fed into the resonator through the m.w. pulse-former unit of the pulsed EPR spectrometer and the TWT amplifier to produce the second pulse in the pulse sequence. EPR samples were illuminated with a 500 W tungsten−halogen lamp through an 8 cm-thick water layer. The Ca^{2+}-depleted S_2 state was produced by illuminating the samples for 1 min at 273 K followed by dark adaptation for 60 min at 273 K based on the abnormal stability of the S_2 state formed in the Ca^{2+}-depleted PS II obtained by the low-pH treatment (*24*, *27*). The membrane samples in the Ca^{2+}-depleted S_2' state were illuminated for further 5 s at 273 K to form the doublet signal, or for a further 1 min at 273 K to form the singlet-like signal (*24*).

Simulation of Doublet Spectra. The spin Hamiltonian for two spins R_1 and R_2 with $S = {}^1/_2$ coupled by the magnetic dipole−dipole interaction (D) and exchange interaction (J) is given by

$$\boldsymbol{H} = g_1\beta\boldsymbol{H}_0S_{1z} + g_2\beta\boldsymbol{H}_0S_{2z} + S_{1z}\sum_j a_{1j}m_{1j} + S_{2z}\sum_j a_{2j}m_{2j} + (-J + D)S_{1z}S_{2z} - (2J + D)(S_1^{+}S_2^{-} + S_1^{-}S_2^{+})/4 \quad (1)$$

where g is the electron g-factor, β is the Bohr magneton, S_1 and S_2 are spins of the coupled radicals,respectively, and $a_{j,k}$ and $m_{j,k}$ are the hyperfine constants and the nuclear spin projection onto the static magnetic field vector ($\boldsymbol{H}_0$), respectively (*24*). The dipole−dipole interaction (D) is defined as $D_0(1 - 3\cos^2\theta)$, where $D_0 = g_1g_2\beta^2/r^3$ and r is the distance between two spins. The exchange interaction (J) is defined as Hamiltonian $\boldsymbol{H}_{\mathrm{exch}} = -J\boldsymbol{S}_1 \cdot \boldsymbol{S}_2$. In the calculation, the hyperfine terms of each spin were represented by a Gaussian line shape (24). In a one-dimensionally oriented sample, the resonance condition, $f(\boldsymbol{H}_0,\alpha)$, derived from eq 1 is averaged over angles θ and φ on polar coordinates and is given by

$$\langle f(\boldsymbol{H}_0,\alpha)\rangle = \int_0^{\pi} \mathrm{d}\theta \int_0^{2\pi} \mathrm{d}\varphi\, f(\boldsymbol{H}_0,\alpha)p(\theta - \theta_0)\sin\theta \quad (2)$$

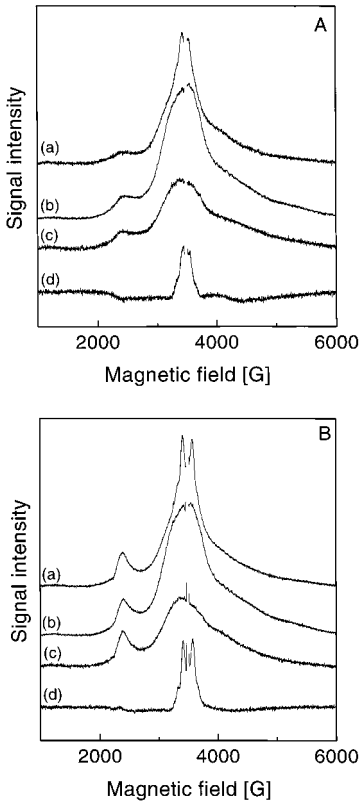

FIGURE 1: Field-swept ESE spectra detected in partially oriented Ca^{2+}-depleted PS II membranes at 0° (panel A) and 90° (panel B) angles between the external magnetic field and the normal of the membrane, respectively. The dark adapted PS II membranes (trace c) were illuminated for 1 min at 273 K followed by dark adaptation for 60 min at 273 K in order to form the Ca^{2+}-depleted S_2 state (trace b), then illuminated for 5 s at 273 K for the formation of the doublet signal (trace a). The spectra of the doublet signal (trace d) were obtained by subtracting the multiline spectra (trace b minus trace c) from the spectra of the multiline plus doublet signal (trace a minus trace c) after adjusting the intensity of the multiline spectra. The center parts of the spectra corresponding to the $Y_D^{\bullet}$ signal were deleted. Primary field-swept ESE conditions; microwave frequency, 9.71 GHz; pulse length, 16 ns for $\pi/2$ pulse and 24 ns for π pulse; $\pi = 200$ ns; pulse repetition rate, 2 ms; temperature, 6 K.

where θ_0 is the angle between the normal of the thylakoid membrane (***n***) and the vector of the external magnetic field ($\boldsymbol{H}_0$), α is the angle between ***n*** and the radius-vector connecting the two radical spins (***r***), and φ is the angle between the projections of $\boldsymbol{H}_0$ and an arbitrary axis onto the membrane plane. $p(\theta - \theta_0)$ is a Gaussian distribution used to evaluate the membrane orientation and is defined by the expression

$$p(\theta - \theta_0) = (2\pi\Delta^2)^{-1/2} \exp[-(\theta - \theta_0)^2/2\Delta^2) \quad (3)$$

where Δ is the mean-square deviation.

RESULTS

Figure 1 shows the field-swept ESE spectra of partially oriented Ca^{2+}-depleted PS II membranes recorded at 0° (panel A) and 90° (panel B) angles between the external magnetic field and the normal of the membrane, respectively. Illuminating the EPR samples for 1 min at 273 K followed by dark adaptation generated the multiline signal (trace b), which is superposed on the cyt b_{559} signal that is present in the dark spectrum (trace c). Illuminating the EPR samples for a further 5 s at 273 K induced a doublet signal at $g \approx 2$ concomitant with a partial decrease in intensity of the multiline signal (trace a). The doublet signals were obtained by subtracting the multiline spectra (trace b minus trace c) from the multiline plus doublet spectra (trace a minus trace c) after adjusting the intensity of the multiline, which was partially decreased concurrent with the formation of the doublet signal (*24*). The doublet and cyt b_{559} signals show a marked angular dependency; the spectra recorded at 0° and 90° are considerably different, whereas the multiline spectra are very similar at the two angles in consistent with the isotropic properties of this signal (*29*). The doublet spectrum (trace d) shows a distinct trough between the peaks at 90° (panel B), but the trough is shallow at 0° (panel A). The anisotropy of the cyt b_{559} signal is due to the perpendicular arrangement of the heme plane with respect to the normal of the thylakoid membranes. This unique arrangement was used as an internal standard to evaluate the orientation of the sample membranes. The value of mean-square deviation (Δ) was determined to be 15° by measuring the angular dependence of the g_z component of the CW spectra of the oxidized cyt b_{559} as described in ref *29* (data not shown).

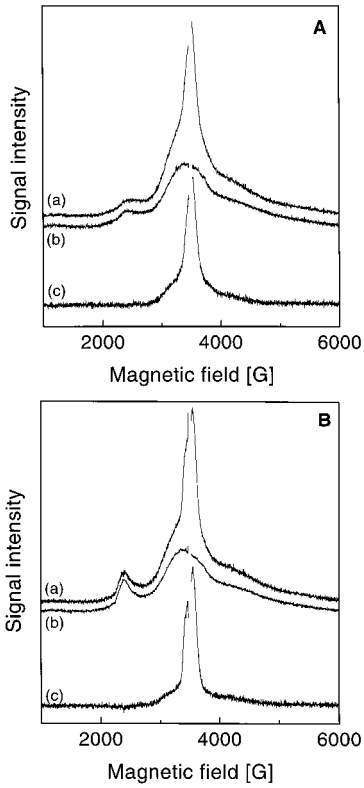

FIGURE 2: Field-swept ESE spectra detected in partially oriented Ca^{2+}-depleted PS II membranes at 0° (panel A) and 90° (panel B) angles between the external magnetic field and the normal of the membrane, respectively. The dark-adapted PS II membranes (trace b) were illuminated for 1 min at 273 K followed by dark adaptation for 60 min at 273 K, then illuminated for 1 min at 273 K (trace a). The singlet-like signal overlapped with the doublet signal (trace c) was obtained by subtracting trace b from trace a. The center parts of the spectra corresponding to the $Y_D^{\bullet}$ signal were deleted. EPR conditions are as described in the Figure 1 legend. See text for other details.

Figure 2 shows the field-swept ESE spectra of partially oriented Ca^{2+}-depleted PS II membranes recorded at 0° (panel A) and 90° (panel B) angles between the external magnetic field and the normal of the membrane. Illuminating

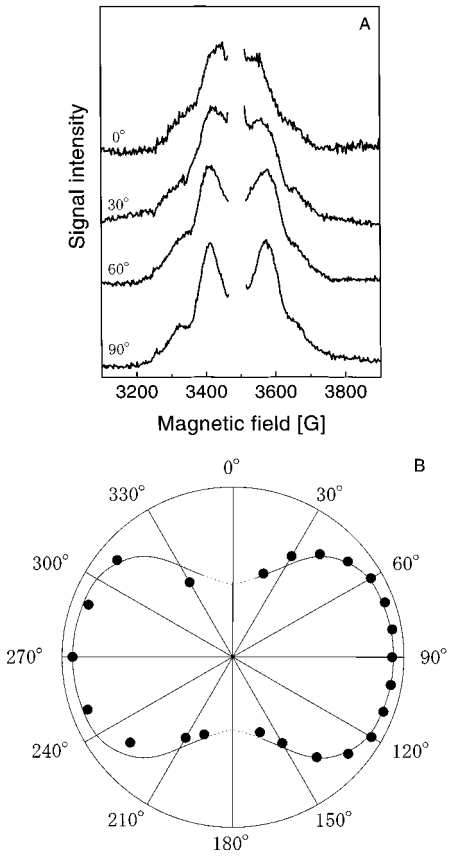

FIGURE 3: Orientation dependence of the doublet signal of the partially oriented Ca^{2+}-depleted PS II membranes (panel A), and the polar-plot (panel B) of the peak-to-peak separation width of the doublet signal in a range of 40−170 G. The numbers represent the angles between the external magnetic field and the normal of the membrane. The center parts of the spectra corresponding to the $Y_D^•$ signal were deleted. EPR conditions are as described in the Figure 1 legend.

Ca^{2+}-depleted PS II in the S_2 state (see trace b in Figure 1) for 1 min at 273 K induces a singlet-like signal concomitant with the disappearance of the multiline signal and partial loss of the doublet signal under the present conditions (trace a). Trace c shows the difference spectra obtained by subtracting the dark adaptation spectra (S_1-state) (trace b) from the illumination spectra (trace a), which consist predominantly of the singlet-like signal. Small but distinct difference was observed between the 0° and the 90° spectra of the singlet-like signal, although the difference is not as pronounced as that of the doublet signal. This may imply that the singlet-like signal is less anisotropic than the doublet signal.

Figure 3 shows the spectra of the doublet signal at 0° (a), 30° (b), 60° (c), and 90°(d) (panel A) and the angular dependency of the splitting width of the spectrum (panel B). Both the separation and depth of trough decrease with decreasing the angle. The results show that the doublet signal has a large magnetic anisotropy, indicating that the doublet signal is attributable to the dipole−dipole interaction between two radicals. This view is compatible with that the doublet signal shows Pake's pattern typical of a pair of $S = {}^1/_2$ spins (*30*).

Figure 4 shows experimental (a, c) and simulated spectra (b, d) of the doublet signal at 0° (A) and 90° (B), respectively. For the simulation, the experimentally obtained Δ angle (15°)

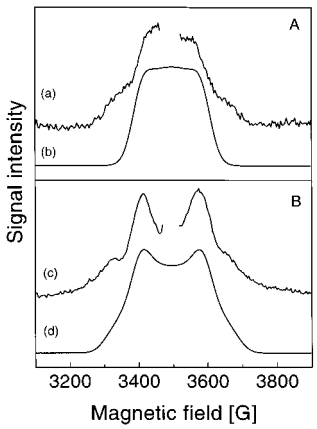

FIGURE 4: Simulation of the doublet signal by a radical pair model. Experimentally obtained spectra (traces a and c), and their simulations (traces b and d) at angles of 0° (panel A) and 90° (panel B) between the external magnetic field and the normal to the membrane. The parameters used for the best fit in simulation were $D_0 = 130$ G, $J = -40$ G, and the Gaussian distribution $\Delta = 15°$ for deviation of orientation. Each spectrum of the radicals was represented by the Gaussian line shape with the width of 20 G (*24*). See text for other details.

and the parameters for magnetic interactions ($D_0 = 130$ G, $J = -40$ G) deduced by simulation of the powder spectrum (*24*) were used. The overall features, the width of doublet-splitting and the angular dependence of the spectra, were well reproduced when the α angle is 65°. The results, therefore, strongly indicate that the dipole−dipole interaction between two organic radicals is the predominant cause of the doublet signal.

To obtain information on the location of the doublet signal center in PS II, the relative arrangement of the doublet species and $Y_D^•$ radical was determined with respect to the thylakoid membranes by measuring ESE-ELDOR spectra for the radical pair composed of the $Y_D^•$ radical and the doublet center in the oriented membranes. For the pulsed ELDOR measurement, the first and third pulses were chosen to produce the ESE signal of the doublet center, while the second pulse was used to invert the magnetic moment of the $Y_D^•$ radical (*31*−*34*). The ESE amplitude depends on the interval between the first and second pulses (*31*−*34*) and is given by the expression

$$\langle V(\tau,\tau')\rangle \propto \int_0^{\pi}\int_0^{2\pi} \mathrm{d}\varphi\ \mathrm{d}\theta\ V(\tau,\tau')p(\theta-\theta_0)\sin\theta \quad (4)$$

$$V(\tau,\tau') \propto 1 - C[1 - \cos(D_{\mathrm{ELD}}\tau')] \quad (5)$$

$$D_{\mathrm{ELD}} = 2\pi g_{\mathrm{A}}\beta g_{\mathrm{B}}\beta/hR^3(1 - 3\cos^2\theta_{\mathrm{R}}) \quad (6)$$

where τ is the time interval between the first and third pulses, τ' is the time interval between the first and second pulses, $p(\theta - \theta_0)$ is the orientation distribution function defined in eq 3, C is the fraction of the $Y_D^•$ radical excited by the second m. w. pulse, D_{ELD} is the dipole interaction between the two spins, and θ_{R} is the angle between the external magnetic field and the radius-vector ($\boldsymbol{R}$) connecting the doublet center with the $Y_D^•$ radical. g_{A} and g_{B} are the g-factors for the doublet center and the $Y_D^•$ radical, respectively, both of which are assumed to be 2. β and h are the Bohr magneton and Plank constant, respectively.

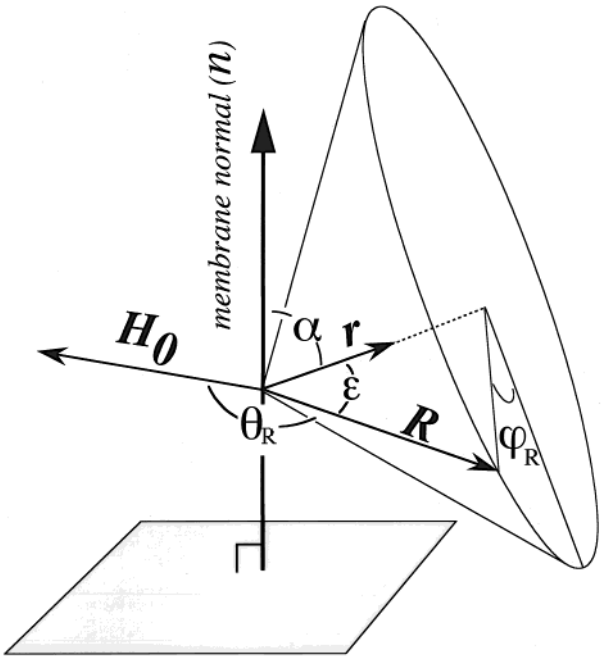

FIGURE 5: Illustration of the relative arrangement between the membrane normal (***n***), radius vector of the radical pair for the doublet signal (***r***), radius vector connecting the doublet signal center with the $Y_D^\bullet$ radical (***R***), and external magnetic field ($\boldsymbol{H}_0$). The vectors are defined by the angles θ_R, α, ϵ, and φ_R. φ_R is the angle required to rotate ***R*** along the circular cone until the angle between ***n*** and ***R*** is equal to the sum of the angles α and ϵ.

As shown in Figure 5, the angles α, ϵ, θ_R, and φ_R define the relative arrangement between the external magnetic field ($\boldsymbol{H}_0$), radius-vector (***R***), and radius-vector (***r***) for the two radicals in the doublet center with respect to the normal of the thylakoid membrane (***n***). The angle α was determined to be 65° by simulating the oriented spectra of the doublet signal in the present study, and the angle ϵ between ***r*** and ***R*** has been estimated to be 70° in a previous study (*33*). φ_R is the angle required to rotate ***R*** along the circular cone until the angle between ***n*** and ***R*** is equal to the sum of the angles of α and ϵ. The relation between these angles is given by the following equation:

$$\cos\theta_R = \sin\theta\cos\varphi\,(\cos\alpha\cos\varphi_R\sin\epsilon + \sin\alpha\cos\epsilon) + \sin\theta\sin\varphi\sin\varphi_R\sin\epsilon + \cos\theta(-\sin\alpha\cos\varphi_R\sin\epsilon + \cos\alpha\cos\epsilon) \quad (7)$$

where the (θ,φ) is the direction of $\boldsymbol{H}_0$ to *Z*-axis, which is taken to be parallel to the membrane normal in polar coordinate system.

Figure 6 shows the experimental (open circles) and the simulated (solid line) ESE ELDOR spectra of partially oriented Ca^{2+}-depleted PS II membranes for the pair spins composed of the $Y_D^\bullet$ radical and the doublet signal center. The spectra were recorded at angles of 0° (panel A) and 90° (panel B) between the external magnetic field vector and the normal of the membrane, where the magnetic field was fixed at the 45 G upfield position from the center of the $Y_D^\bullet$ radical signal (inset figure). The resulting spectra showed pronounced angular dependency and the spectra at 0° and 90° were considerably different. The lines for best fit simulation of both spectra were obtained when φ_R is 71°.

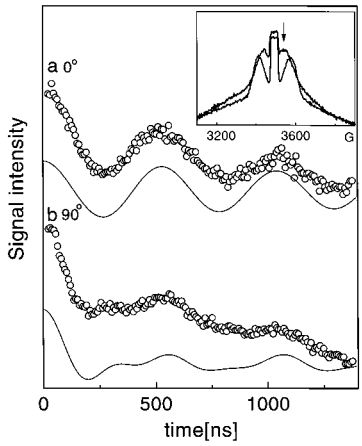

FIGURE 6: ESE-ELDOR spectra detected in partially oriented Ca^{2+}-depleted PS II membranes at 0° (a) and 90° (b) angles between the external magnetic field and the normal of the membrane (open circles), and their simulations (solid line). The sample membranes were illuminated for 5 s at 273 K for the formation of the doublet signal as described in the Figure 1 legend. The magnetic field was fixed at the 45 G upfield position from the center of the $Y_D^\bullet$ radical indicated by an arrow in the inset figure. ESE-ELDOR conditions: first and third pulses, 9.75 GHz; second pulse, 9.85 GHz; τ, 1400 ns; $\boldsymbol{H}_0$, 3532 G; temperature, 6 K

DISCUSSION

The results of the present study indicate that the oriented field-swept ESE spectra of the doublet signal is well reproduced by the dipole−dipole and exchange interactions which are consistent with those determined by simulation of powder spectra (*24*). The results are compatible with the view that an organic radical pair is responsible for the doublet signal. The results of the present study also provide information on the angle α (=65°) between the radius-vector (***r***) of the radical pair for the doublet signal and the normal of the thylakoid membrane, and the angle φ_R (=71°) (see Figure 5). These angles and the reported angle ϵ (=70°) between the ***r*** vector and the ***R*** vector connecting the $Y_D^\bullet$ radical with the doublet signal center, as well as the reported distances between the doublet signal center and the $Y_D^\bullet$ radical (29.7 Å), and between the two radicals for the doublet signal center (5.3 Å) allow us to derive the relative arrangement of the doublet signal center in PS II.

A schematic model of the arrangement of the doublet signal center in PS II is illustrated in Figure 7, where the XZ and XY planes correspond to the plane including the radius vector of the radical pair for the doublet signal (***r***) and the plane of the thylakoid membranes, respectively. β is the angle between the projection of the ***R*** vector on the membrane plane and X-axis, and γ is the angle between the ***R*** vector and the membrane plane. The angles β and γ are a function of the angles α, φ_R, and ϵ:

$$\beta = \tan^{-1}\{(\cos\alpha\cos\varphi_R\sin\epsilon + \sin\alpha\cos\epsilon)/\sin\varphi_R\sin\epsilon\}$$

$$\gamma = \sin^{-1}(\sin\alpha\cos\varphi_R\sin\epsilon - \cos\alpha\cos\epsilon)$$

and are determined to be 64° and 8°, respectively. The vector ***R*** connecting the $Y_D^\bullet$ radical and the doublet signal center has a distance of 29.7 Å and tilts by 8° with respect to the membrane plane, indicating that the vector is almost parallel

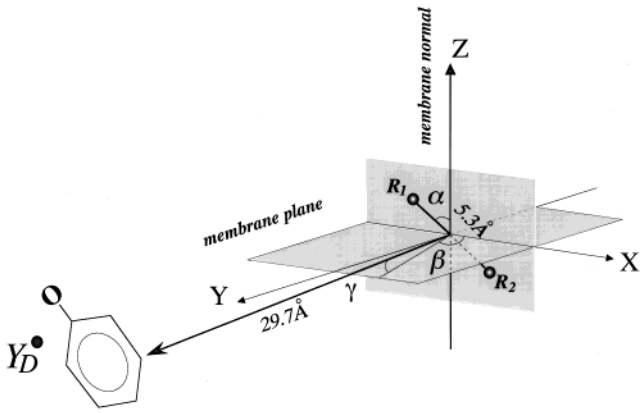

FIGURE 7: A model of the arrangement of the doublet signal center in PS II based on the results of the present study ($\alpha = 65°$, $\beta = 64°$, and $\gamma = 8°$) and the results of previously reported studies ($r = 5.3$ Å and $R = 29.7$ Å) (*24*, *33*). The XZ plane was chosen to include the radius vector of the radical pair for the doublet signal (***r***), while the thylakoid membrane was taken as the XY plane. See text for other details.

to the thylakoid membranes. Notably, these values coincide well with the distance between the Y_D and Y_Z tyrosine (=30 Å), and the angle between the Y_D-Y_Z vector and the membrane plane (=10°) (*34*). These results lead us to believe that the $Y_Z^\bullet$ radical is the counterpart of the radical pair for the doublet signal center. Furthermore, this view is compatible with the result deduced by pulsed ENDOR-induced EPR measurement that shows the association of the $Y_Z^\bullet$ radical to the doublet signal (*24*).

Detailed analysis on the split signal observed at the $g = 2.0$ region have been reported in acetate-treated PS II membranes (*16*, *20*−*22*, *35*−*39*). However, the obtained results and conclusions of these studies are not necessarily consistent with each other. Reported ESE field-swept spectra of the split-signal in the acetate treated PS II differ considerably according to study (*21*, *22*): the signal obtained by Force et al. (*21*) was similar to the doublet signal and was simulated mainly by dipole interaction, whereas the signal obtained by Peloquin et al. (*22*) was rather similar to the singlet-like signal and was simulated mainly by exchange interaction. Taking into account the results obtained in Ca^{2+}-depleted PS II, these can be reconciled if the doublet and singlet-like signals are induced with variously different ratio in the $g = 2$ region to yield a split signal in acetate-treated PS II. In fact, the sample membranes were illuminated for 5−60 s at room temperature in the absence of DCMU (*21*, *22*, *35*−*39*), which conditions may result in both the doublet and the singlet-like signals that overlap in the $g = 2.0$ region in Ca^{2+}-depleted PS II. Our preliminary result shows that illuminating the acetate-treated PS II membranes for 6 s in the absent of DCMU, the conditions which induce the doublet signal in Ca^{2+}-depleted PS II, generates a doublet signal (data not shown). These considerations lead us to the view that the doublet signal could be induced by illuminating the Ca^{2+}-depleted and acetate-treated PS II, although the fraction of the signal will depend on the sample preparations and the illumination conditions.

The high-frequency pulsed ENDOR study of the split-signal in acetate-treated PS II indicates the involvement of the Mn-cluster in the signal, which has been simulated by a large exchange interaction between the Mn-cluster with $S = {}^1/_2$ and a radical with $S = {}^1/_2$. The latter $S = {}^1/_2$ radical has been assigned to the $Y_Z^\bullet$ radical based on the similarity between the pulsed ENDOR spectra of the split-signal and the $Y_Z^\bullet$ signal (*19*), and the modification of the ESEEM spectra of the split-signal by labeling of deuterated tyrosine (*20*). On the other hand, the pulsed ENDOR-induced EPR study shows that the $Y_Z^\bullet$ radical is associated only with the doublet signal in Ca^{2+}-depleted PS II (*24*). Therefore, we may assume that the $Y_Z^\bullet$ radical found in the split signal in acetate-treated PS II is caused by the doublet signal, and that the Mn-cluster is associated with the other singlet-like signal. The dipole interaction between the $Y_Z^\bullet$ radical and the other radical is responsible for the doublet signal, while the interaction between the Mn-cluster and an unknown radical is responsible for the singlet-like signal, respectively. The latest simulation study of the split-signal in acetate-treated PS II by Peloquin et al. (*22*) has indicated that the distance between the Mn-cluster and the putative radical is 8.6−11.5 Å, which was assigned to the distance between the Mn-cluster and the $Y_Z^\bullet$ radical. However, it may be possible to assume that the distances may reflect that between the Mn-cluster and the putative radical other than the $Y_Z^\bullet$ radical since the contribution of the doublet signal to the obtained split signal seems to be small because of the similarity of the split signal to the singlet-like signal.

Detail simulation studies of split signal obtained by CW EPR experiments in acetate treated PS II revealed that the spectrum is reproduced by using a large exchange interaction with a small dipole interaction (*36*−*39*). However, it should be noted that the integration of the obtained and simulated CW split spectra (*35*, *36*, *38*) cannot reproduce the reported ESE field swept absorption spectra (*21*, *24*). Although we cannot define the precise reason for the marked inconsistency between the spectra obtained by CW and pulsed EPR measurements at present, it may be rational to consider that the split spectra in CW measurements are inhomogeneously broadened by the local fields, while it does not influence spin−echo intensity in pulsed measurement.

At present, little is known about the origin of each radical species, which is the counterpart of the $Y_Z^\bullet$ radical to form the doublet signal or the counterpart of the Mn-cluster to form the singlet-like signal. It has been suggested that His190 of the D1 protein closely associates with the photoassembly of the Mn-cluster and may be functionally involved in oxygen evolution (2). Furthermore, a structural model of the D1/D2 protein based on the apparent homology with the L/M reaction center of the photosynthesis bacterium as well as energy calculation claims that His 190 is also located close proximity to the Y_Z tyrosine (*40*). The histidine radical of D1−190 can, therefore, be a possible candidate for the putative radical species responsible for the doublet signal or singlet-like signal, although how this can be achieved has not been resolved. Further studies will be necessary in order to clarify the origin and function of the putative radicals.

REFERENCES

1. Rutherford, A. W., Zimmermann, J.-L., and Boussac, A. (1992) *The Photosystems: Structure, Function and Molecular Biology* (Barber, J., Ed.) pp 179−229, Elsevier, Amsterdam.
2. Debus, R. J. (1992) *Biochim. Biophys. Acta 1102*, 269−352
3. Sauer, K., Yachandra, V. K., Britt, R. D., and Klein, M. P. (1992) *Manganese Redox Enzymes* (Pecoraro, V. L., Ed.) pp 105−118, VCH, New York.

4. Britt, R. D. (1996) *Oxygen Photosynthesis: The Light Reaction* (Ort, D. R., and Yocum, C. F., Ed.) pp 137−164, Kluwer Academic Publisher.
5. Ono, T., Noguchi, T., Inoue, Y., Kusunoki, M., Matsushita, T., and Oyanagi, H. (1992) *Science 258*, 1335−1337.
6. Roelofs, T. A., Liang, W., Latimer, M. J., Cinco, R. M., Rompel, A., Andrews, J. C., Sauer, K., Yachandra, V. K., and Klein, M. P. (1996) *Proc. Natl. Acad. Sci. U.S.A. 93*, 3335−3340.
7. Latimer, M. J., DeRose, V. J., Mukerji, I., Yachandra, V. K., Sauer, K., and Klein. M. P. (1995) *Biochemistry 34*, 10898−10909.
8. Noguchi, T., Ono, T., and Inoue, Y. (1995) *Biochim. Biophys. Acta 1228*, 189−200.
9. Ono, T. Noguchi, T., Inoue, Y., Kusunoki, M., Yamaguchi, H., and Oyanagi, H. (1993) *FEBS Lett. 330*, 28−30.
10. Sivaraja, M., Tso, J., and Dismukes, G. C. (1989) *Biochemistry 28*, 9459−9464.
11. Tso, J., Sivaraja, M., Philo, J. S., and Dismukes, G. C. (1991) *Biochemistry 30*, 4740−4747.
12. Ono, T., and Inoue, Y. (1990) *Biochim. Biophys. Acta 1015*, 373−377.
13. Boussac, A., and Rutherford, A. W. (1988) *Biochemistry 27*, 3476−3483.
14. Boussac, A., Zimmermann, J -L., and Rutherford, A. W. (1989) *Biochemistry 28*, 8984−8989.
15. Matsukawa, T., Mino, H., Yoneda, D., and Kawamori, A. (1999) *Biochemistry 38*, 4072−4077.
16. Hallahan, B. J., Nugent, J. H., Warden, J. T., and Evans, M. C. (1992) *Biochemistry 31*, 4562−4573
17. Boussac, A., Zimmermann, J.-L., Rutherford, A. W., and Lavergne, J. (1990) *Nature 347*, 303−306.
18. Berthomieu, C., and Boussac, A. (1995) *Biochemistry 34*, 1541−1548.
19. Gilchrist, M. L. Jr., Ball, J. A., Randall, D. W., and Britt, R. D. (1995) *Proc. Natl. Acad. Sci. U.S.A. 92*, 9545−9549.
20. Tang, X.-S., Randall, D. W., Force, D. A., Diner, B. A., and Britt, R. D. (1996) *J. Am. Chem. Soc. 118*, 7638−7639.
21. Force, D. A., Randall, D. W., and Britt, R. D. (1997) *Biochemistry 36*, 12062−12070.
22. Peloquin, J. M., Campbell, K. A., and Britt, R. D. (1998) *J. Am. Chem. Soc. 120*, 6840−6841.
23. Hoganson C. W., and Babcock G. T. (1997) *Science 277*, 1953−1956.
24. Astashkin, A. V., Mino, H., Kawamori, A., and Ono, T. (1997) *Chem. Phys. Lett. 272*, 506−516.
25. Berthold, D. A., Babcock, G. T., and Yocum, C. F. (1981) *FEBS Lett. 134*, 231−234.
26. Ono, T., and Inoue, Y. (1986) *Biochim. Biophys. Acta 850*, 380−389.
27. Ono, T., and Inoue, Y. (1989) *Biochim. Biophys. Acta 973*, 443−449.
28. Mino, H., Kawamori, A., Matsukawa, T., and Ono, T. (1998) *Biochemistry 37*, 2794−2799.
29. Hasegawa, K., Kusunoki, M., Inoue, Y., and Ono, T. (1998) *Biochemistry 37*, 9457−9465.
30. Pake, G. E. (1948) *J. Chem. Phys. 16*, 327−336.
31. Milov, A. D., Salikhov, K. M., and Shirov, M. D. (1981) *Fiz. Tverd. Tela 23*, 975−982.
32. Milov, A. D., Ponomarev, A. B., and Tsvetkov, Yu. D. (1984) *Chem. Phys. Lett. 110*, 67−72.
33. Hara, H., Kawamori, A., Astashkin, A. V., and Ono, T. (1996) *Biochim. Biophys. Acta 1276*, 140−146.
34. Astashkin, A. V., Hara, H., and Kawamori, A. (1998) *J. Chem. Phys. 108*, 3805−3812.
35. Szalai, V. A., and Brudvig, G. W. (1996) *Biochemistry 35*, 1946−1953.
36. Lakshmi, K. V., Eaton, S. S., Eaton G. R., Frank, H. A. And Brudvig, G. W. (1998) *J. Phys. Chem. B 102*, 8327−8335.
37. Lakshmi, K. V., Eaton, S. S., Eaton, G. R., and Brudvig, G. W. (1999) *Biochemistry 28*, 12758−12767.
38. Dorlet, P., Valentin, M. D., Babcock, G. T., and McCracken, J. L. (1998) *J. Phys. Chem. B, 102*, 8239−8247.
39. Dorlet, P., Boussac, A. Rutherford, A. W., and Un, S. (1999) *J. Phys. Chem. B, 103*, 10945−90954.
40. Svensson, B., Vass, I., and Styring, S. (1991) *Z. Naturforsch., 46c*, 765−776.

BI9929406